

# Discovery potential of the SM Higgs with ATLAS \*

P. Fleischmann<sup>†</sup>

On behalf of the ATLAS Collaboration

1st October 2009

## Abstract

The discovery potential of the Standard Model Higgs boson with the ATLAS experiment at the Large Hadron Collider is reviewed for the HEP-MAD'09 conference. The Higgs decay channels  $b\bar{b}$ ,  $\tau^+\tau^-$ ,  $\gamma\gamma$ ,  $WW^{(*)}$  and  $ZZ^{(*)}$  are discussed. The results of the combination of the individual analyses to obtain the discovery potential and exclusion limits are also presented.

## 1 Introduction

The ATLAS detector [1] is a general purpose detector at the Large Hadron Collider (LHC), the new particle accelerator at CERN in Geneva. The first collisions of protons are scheduled for the end of 2009. The design centre-of-mass energy for the two proton beams is 14 TeV. One of the prime tasks for the ATLAS experiment is the search for the Standard Model (SM) Higgs boson. The search will be performed at different ranges of possible Higgs masses using various decay channels [2]. In addition to each individual analysis the obtained results will also be combined to enhance the significance.

The Higgs boson is the missing keystone of the Standard Model of particle physics. A lower bound to the mass of this particle has been set by the LEP experiments [3]. They exclude at a 95% confidence level the mass region below 114.4 GeV, where most of the region is excluded at an even higher confidence level. More recently the experiments at the Tevatron have published results that exclude an additional region between 160 GeV and 170 GeV [4].

All results of the ATLAS Collaboration presented here have been obtained using Monte Carlo simulations corresponding to the LHC's design centre-of-mass energy of 14 TeV. In the current run schedule it is foreseen to start with a lower energy of about 7 TeV, that will be increased during the first year of operations to 10 TeV and afterwards to the design value. In some first on-going studies it has been found, that the amount of integrated luminosity as mentioned in the results of the analyses at 14 TeV have to be multiplied by a factor of about 2 to get similar results for a centre-of-mass energy of the two proton beams of 10 TeV.

In section 2 a brief overview of the production and decay channels for a SM Higgs boson as expected at the LHC is given. In section 3 the prepared analyses of the decay channels most relevant for the discovery of the SM Higgs boson are described. Section 4 summarises the effort to combine the results of various analyses in order to increase the significance of a potential signal or exclusion limits.

---

\*Talk presented at the conference HEP-MAD'09, 21-28th August 2009, Antananarivo, Madagascar

<sup>†</sup>Universität Würzburg

## 2 The SM Higgs boson at the LHC

The production cross-section of the SM Higgs boson in proton-proton collisions depends on the Higgs mass and centre-of-mass energy. Figure 1(a) shows the cross-sections for five production channels at the LHC. The dominant process at the LHC is the production via gluon fusion followed by the Vector Boson Fusion (VBF). At much lower rates the associated production with a Vector Boson ( $HW$  and  $HZ$ ) or a  $t\bar{t}$ -pair contributes to the total production cross-section.

The search for the SM Higgs boson is performed at the LHC in various decay channels. The signal rates and the signal to background ratios of each channel depend on the Higgs mass. Figure 1(b) shows the branching ratios for decay modes of a SM Higgs boson as a function of the Higgs mass. At low masses of the Higgs boson the decay  $H \rightarrow b\bar{b}$  has the highest branching ratio, but also the decays into  $\tau^+\tau^-$  or  $\gamma\gamma$  plays an important role. At intermediate and higher Higgs masses the relevance of the decays  $H \rightarrow WW^{(*)} \rightarrow \ell\nu\ell\nu$  and  $H \rightarrow ZZ^{(*)} \rightarrow 4\ell$  increases. The SM Higgs decay into  $t\bar{t}$  is not considered here since the experimental results up to now favour a not too high Higgs mass.

## 3 Decay channels for the SM Higgs boson search

In this section the most relevant decay channels for a discovery of the SM Higgs boson are overviewed. A more detailed description of each analysis can be found elsewhere [2].

### 3.1 $t\bar{t}H \rightarrow t\bar{t}b\bar{b}$

The dominant decay mode for a low mass Higgs ( $m_H < 130$  GeV) is the decay  $H \rightarrow b\bar{b}$ . However it is very difficult to measure, since the expected signal sits on top of a large QCD background (see Figure 2(a)). It is therefore important to look for a noticeable signature. In the ATLAS Collaboration the process  $t\bar{t}H \rightarrow t\bar{t}b\bar{b}$  has been investigated, where the top quark predominantly decays into  $Wb$ . Thus, the final state contains at least four  $b$ -jets. Figure 2(b) shows an example of a Feynman diagram for the  $t\bar{t}H$  channel, where one of the  $W$  bosons decays leptonically, while the other decays hadronically.

Due to the challenges in the decay mode, this channel is not considered the most important channel for the discovery of the SM Higgs boson. However this channel grants access to some parameters of the Higgs boson which will be important to measure, once it has been discovered. In addition it has recently been found [5], that this decay mode is reinstated as a promising search channel if one performs an exclusive analysis of the high  $p_T$  region of the  $HW$  and  $HZ$  production.

### 3.2 $H \rightarrow \tau^+\tau^-$

The Higgs decay into a pair of  $\tau$  leptons is another important channel in the low mass region. Though it has a lower branching ratio than the decay  $H \rightarrow b\bar{b}$ , it provides a clean signature in the VBF production channel. The characteristics of the VBF are two high  $p_T$  jets at large pseudo-rapidity with only little hadronic activity in the central region (rapidity gap). Figure 3 shows the pseudo-rapidity distributions for the two jets with the highest  $p_T$ . In this analysis three decay modes of the  $\tau^+\tau^-$ -pair are considered: hadron-hadron ( $hh$ -channel), lepton-hadron ( $\ell h$ -channel) and lepton-lepton ( $\ell\ell$ -channel). The signal events are selected using the VBF signature characteristics as well as the requirement of a  $\tau^+\tau^-$ -pair from a resonance and missing transverse energy  $E_T^{\text{miss}}$ . The Higgs mass is reconstructed using a collinear approximation for the  $\tau$  decays, which assumes, that the decay products are emitted in the same direction as the  $\tau$ .

The dominant background for this process is  $Z$ -jets with the  $Z$  decaying into a pair of  $\tau$  leptons. The Higgs mass peak is sitting in the tail of the  $Z \rightarrow \tau^+\tau^-$  distribution as shown in Figure 4(a). Since the resolution of the reconstructed Higgs mass is limited by the knowledge of the  $E_T^{\text{miss}}$  and the  $\tau$ -reconstruction, it is essential to know the shape of the background distribution. A data-driven

method has been established to estimate the shape of the  $m_{Z \rightarrow \tau\tau}$  distribution by using  $Z \rightarrow \mu^+ \mu^-$  data where the  $\mu$  is replaced by simulated  $\tau$  leptons. The expected sensitivity using only the  $\ell\ell$ - and the  $\ell h$ -channel is presented in Figure 4(b). The  $hh$ -channel is not used in the combination as it suffers from uncertainties on the large QCD background.

### 3.3 $H \rightarrow \gamma\gamma$

Another Higgs decay mode relevant at low masses of the Higgs boson is the decay into a pair of photons. It has a rather small branching ratio, however it has a distinctive signature of two high  $p_T$  photons forming a resonance on top of a smooth background (Figure 5). The biggest contribution to the large background comes from the irreducible direct  $\gamma\gamma$  production. A good rejection power is needed to keep the fraction of  $\gamma$  + jet events low, where at least one particle is misidentified as photon. To achieve this a cut on shower shape parameters is applied to reject pions which are the main source of fake photons. In addition track isolation cuts are applied to further reduce fake background.

Beside the inclusive analysis also exclusive searches for the  $H \rightarrow \gamma\gamma$  decay in association with no, one or two jets are performed. Figure 6(a) shows an examples for the invariant mass distribution for the analysis requiring two jets. It has been found, that the combination of the results of the exclusive analyses shows a higher significance than the result of the inclusive search (Figure 6(b)).

### 3.4 $H \rightarrow WW^{(*)} \rightarrow \ell\nu\ell\nu$

The SM Higgs boson decay into a pair of  $W$  bosons has a large branching ratio over a wide range of  $m_H$ . Two separate analyses are being performed for the gluon fusion and the VBF. In contrast to the other Higgs decay channels presented here one cannot reconstruct the Higgs boson due to the neutrinos in the decay  $WW^{(*)} \rightarrow \ell\nu\ell\nu$ , thus only the transverse mass is accessible (Figure 7). Currently only the decay into  $e\nu\mu\nu$  is used in the combination of the different Higgs searches, but other studies are on-going. The analyses are based on event counting and rely on a good understanding of the background shape and normalisation. The main contributions to the background originate from production of  $WW$ ,  $t\bar{t}$  and  $W$ +jets. Due to the correlated spins of the two  $W$  bosons the decay leptons go preferentially in the same direction. This fact can be used to suppress the  $WW$  background and to select a background-enhanced control sample to determine the background normalisation (Figure 8). The  $t\bar{t}$  background can be suppressed by a jet veto in the central region. Cuts on the lepton isolation can be used to reduce the amount of  $W$ +jets events.

### 3.5 $H \rightarrow ZZ^{(*)} \rightarrow 4\ell$

The Higgs decay into four leptons is often referred to as the *golden channel* for the search of a SM Higgs boson with a mass above 130 GeV. It has a smaller branching ratio as the  $H \rightarrow WW^{(*)}$  channel, but due to its clean experimental signature it is considered the most promising channel except for a region around  $m_H \approx 2M_W$  where the decay  $H \rightarrow WW^{(*)}$  dominates the other modes. The signal can be observed as a narrow resonance on top of a broad background, which is dominated by the  $ZZ$  production. Figure 9 shows two example of the expected invariant mass distribution for two different values of the Higgs mass. Beside the  $ZZ$  background there are also contributions from  $Zb\bar{b}$  and  $t\bar{t}$ . There are currently large theoretical uncertainties on their production cross sections. Therefore it is important to suppress these processes by selection criteria to a rate well below the irreducible  $ZZ$  background. Due to the longer lifetime of the heavy quarks, leptons from the  $Zb\bar{b}$  and  $t\bar{t}$  background originate from secondary vertices and can thus be suppressed by cuts on the impact parameter significance. In addition requirements on the lepton track isolation in the tracker and calorimeter can further reduce the amount of these background processes.

This study is being performed in three sub-channels:  $4e$ ,  $4\mu$  and  $2e2\mu$ . The Higgs mass can be fully reconstructed. However with four leptons in the final state a good single lepton reconstruction

and trigger efficiency is essential. Figure 10 shows the expected selection efficiency in the three channels as well as the signal significance as a function of the Higgs mass.

## 4 Higgs discovery potential and exclusion limits

Some of the presented decay channels will allow to reach a  $5\sigma$  discovery already stand-alone in parts of the mass range. In order to further increase the sensitivity over a wider range of Higgs mass values several of the individual results are combined using a method based on the profile likelihood ratio. The channels currently used are  $H \rightarrow \tau^+\tau^-$ ,  $H \rightarrow \gamma\gamma$ ,  $H \rightarrow WW^{(*)}$  and  $H \rightarrow ZZ^{(*)}$ . The results presented here use a fixed-mass hypothesis, however studies where the Higgs mass is regarded as a free parameter are on-going. Figure 11 shows the expected signal significance and exclusion limits for different Higgs masses and different values of integrated luminosity. One can see that in some regions of the Higgs mass it is expected to be able to reject it or see a signal already with  $2\text{fb}^{-1}$ .

## 5 Acknowledgements

The author would like to thank all ATLAS collaborators. Special thanks to Ketevi Assamagan, Bill Murray and other colleagues of the Higgs Working Group for their useful comments and suggestions.

## References

- [1] ATLAS Collaboration, G. Aad et al., *The ATLAS Experiment at the CERN Large Hadron Collider*, JINST **3** (2008) S08003.
- [2] ATLAS Collaboration, G. Aad et al., *Expected Performance of the ATLAS Experiment - Detector, Trigger and Physics*, arXiv:0901.0512 [hep-ex].
- [3] LEP Higgs boson search Collaboration, R. Barate et al., *Search for the standard model Higgs boson at LEP*, Phys. Lett. **B565** (2003) 61–75, arXiv:0306033 [hep-ex].
- [4] TEVNPH Collaboration, *Combined CDF and DZero Upper Limits on Standard Model Higgs-Boson Production with up to 4.2 fb-1 of Data*, arXiv:0903.4001 [hep-ex].
- [5] *ATLAS Sensitivity to the Standard Model Higgs in the HW and HZ Channels at High Transverse Momenta*, Tech. Rep. ATL-PHYS-PUB-2009-088. ATL-COM-PHYS-2009-345, CERN, Geneva, Aug, 2009.

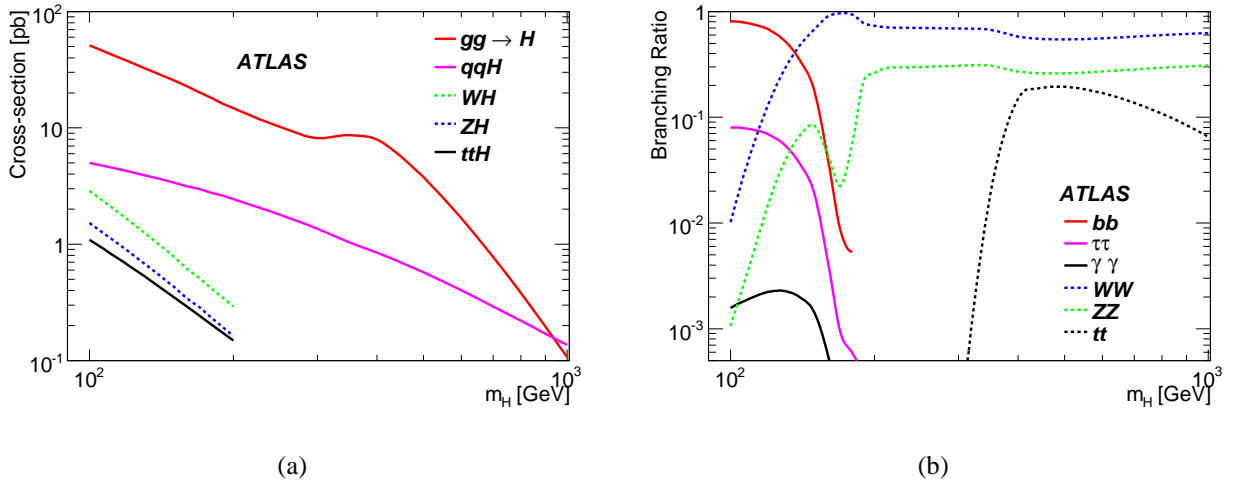


Figure 1: (a) Cross-sections for the five production channels of the SM Higgs boson at the LHC as a function of its mass. (b) Branching ratios for the most relevant decay modes of the SM Higgs boson as a function of its mass.

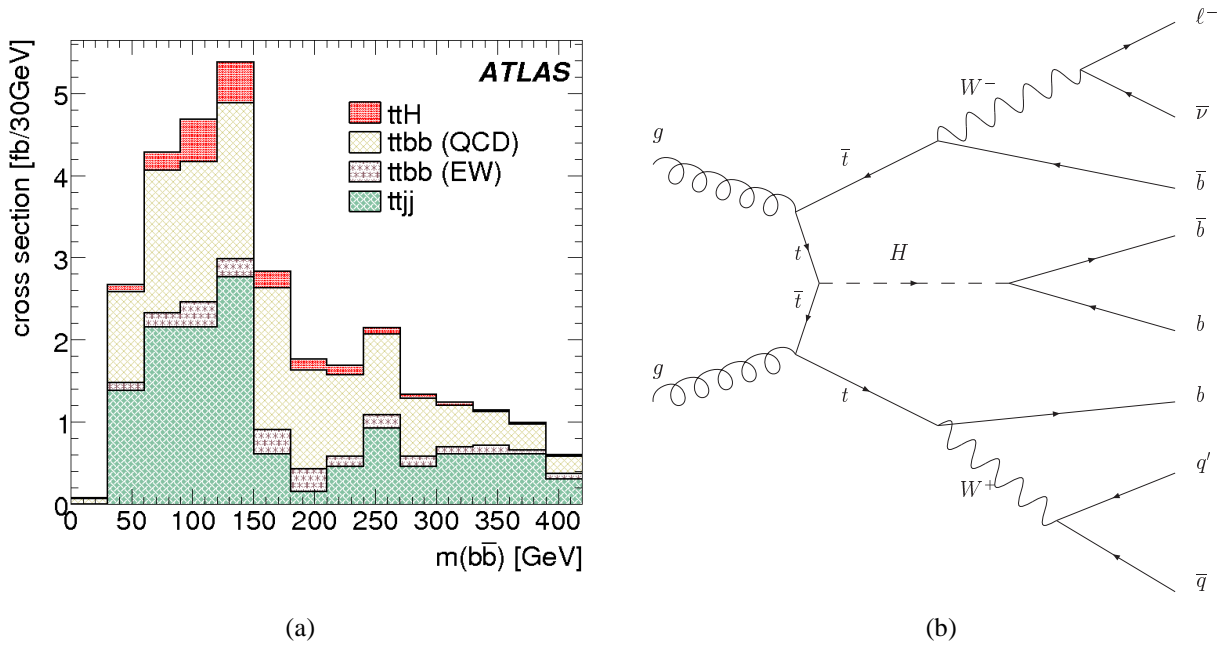
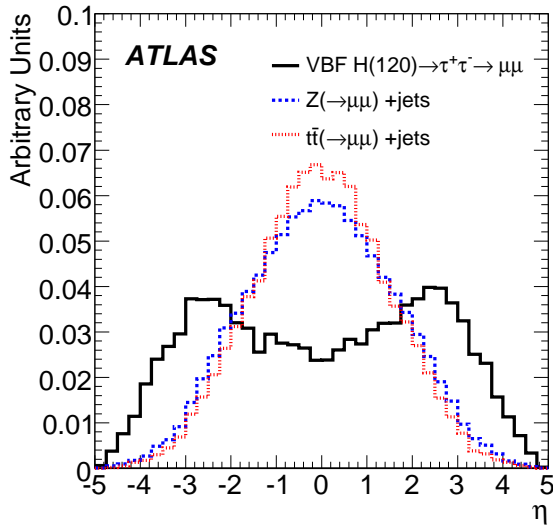
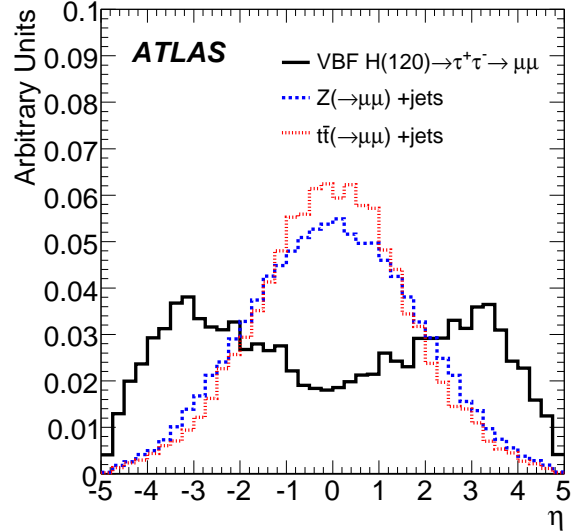


Figure 2: (a) Reconstructed invariant mass spectrum for signal and backgrounds in the  $t\bar{t}H \rightarrow t\bar{t}b\bar{b}$  channel. (b) One of the Feynman diagrams for the  $t\bar{t}H$  production where the Higgs boson decays into  $b\bar{b}$ . Here one top quark decays hadronically, while the other decays leptonically.

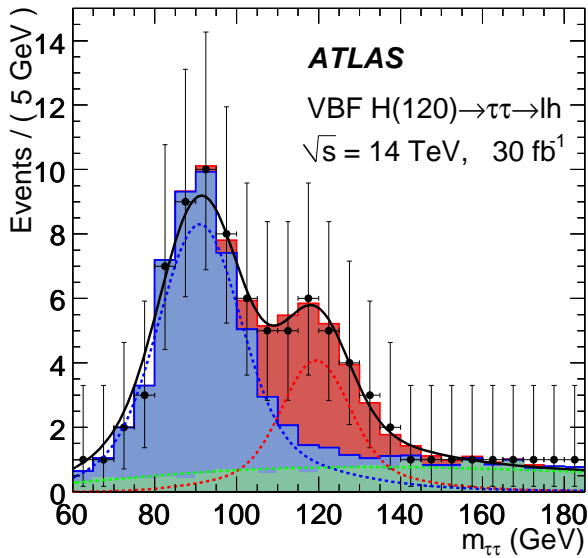


(a)

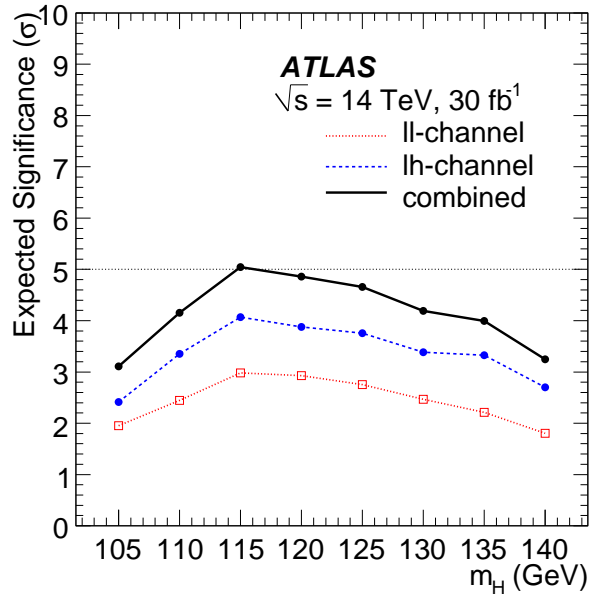


(b)

Figure 3: Pseudo-rapidity of the (a) highest  $p_T$  and (b) the second highest  $p_T$  jets in the VBF process  $H \rightarrow \tau\tau \rightarrow \mu\mu$  and backgrounds.

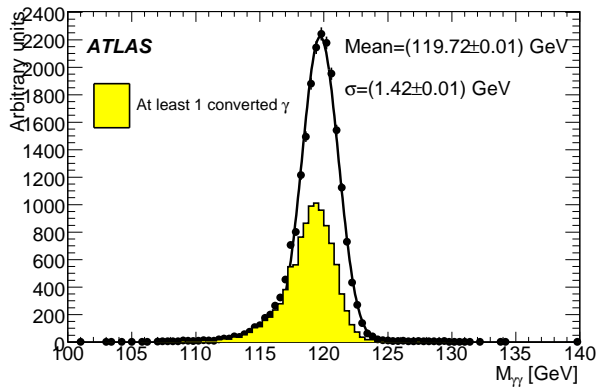


(a)

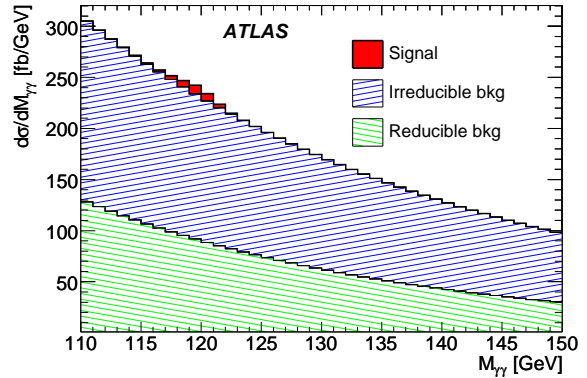


(b)

Figure 4: (a) Example of the reconstructed invariant mass spectrum for signal and backgrounds in the  $H \rightarrow \tau\tau$  channel for a SM Higgs boson of mass  $m_H = 120$  GeV based on an integrated luminosity of  $30\text{fb}^{-1}$ . (b) Expected signal significance for the  $H \rightarrow \tau\tau$  channel as a function of the Higgs mass.

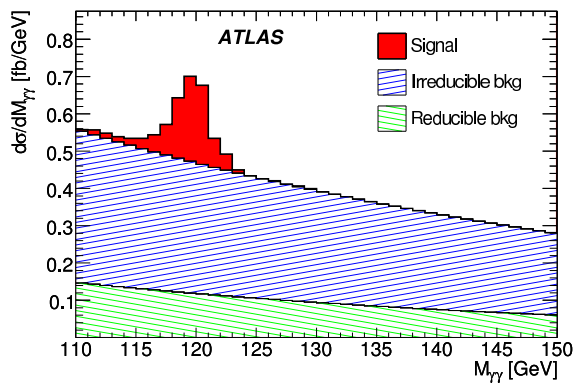


(a)

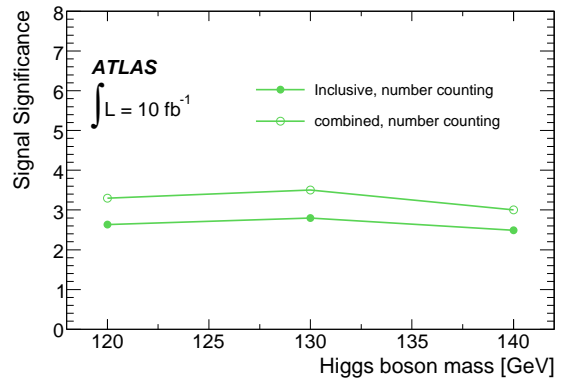


(b)

Figure 5: (a) Invariant mass distribution for photon pairs from Higgs boson decays with  $m_H = 120$  GeV after trigger and identification cuts. The shaded histogram correspond to events with at least one converted photon. (b) Invariant mass distribution for signal and backgrounds in the inclusive  $H \rightarrow \gamma\gamma$  channel.

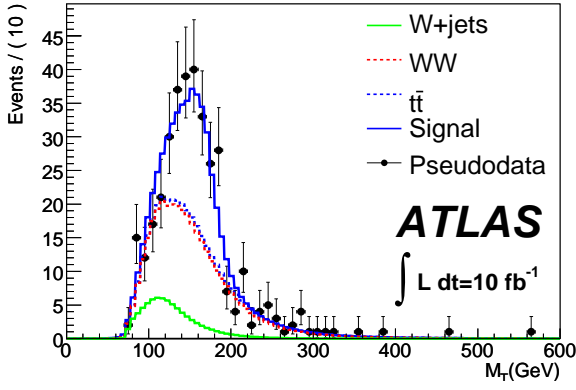


(a)

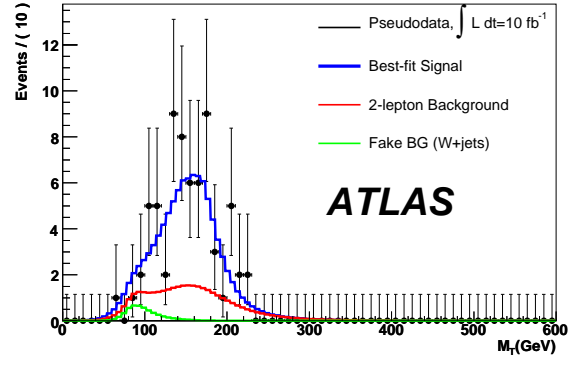


(b)

Figure 6: (a) Invariant mass distribution for signal and backgrounds in the exclusive  $H \rightarrow \gamma\gamma$  channel requiring two jets. (b) Expected signal significance for a Higgs boson using the  $H \rightarrow \gamma\gamma$  decay for  $10 \text{ fb}^{-1}$  of integrated luminosity as a function of the mass. The solid circles correspond to the sensitivity of the inclusive analysis while the open circles display the significance when the Higgs boson plus jet analyses are included.

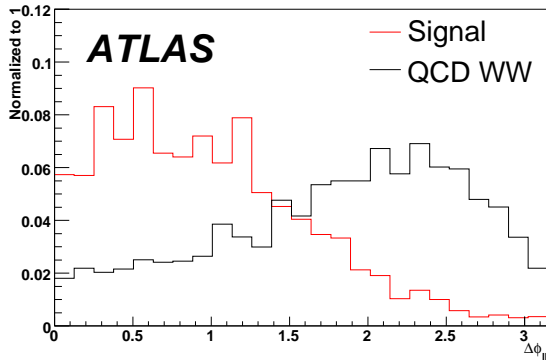


(a)

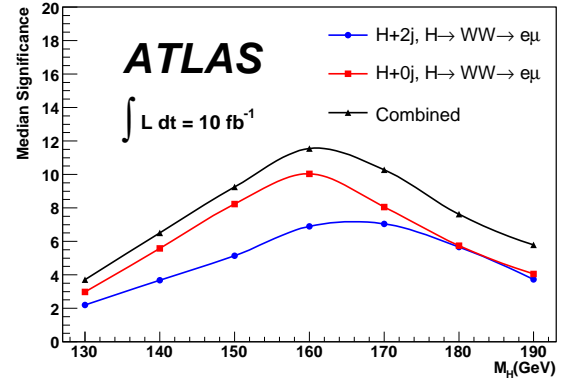


(b)

Figure 7: Expected distribution of the transverse mass  $M_T$  for signal and backgrounds in the  $H \rightarrow WW^*$  channel requiring (a) no jets (b) two jets for an integrated luminosity of  $10\text{fb}^{-1}$ .

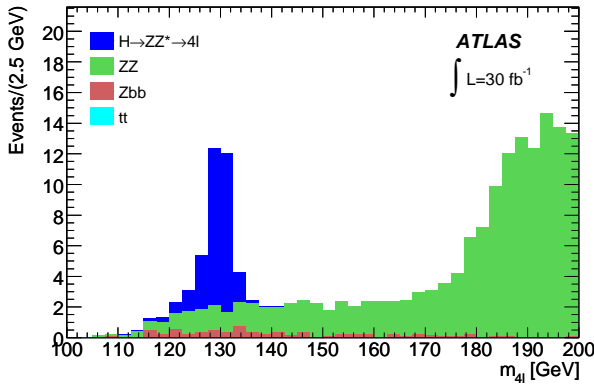


(a)

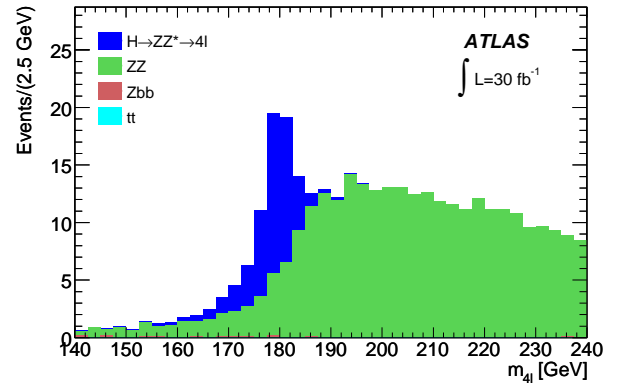


(b)

Figure 8: (a) Normalised distribution of the opening angle  $\Delta\phi_{\ell\ell}$  between the two leptons in signal and background events of the  $H \rightarrow WW^*$  channel. (b) Expected signal significance as a function of the Higgs mass for the  $H \rightarrow WW^*$  channel based on  $10\text{fb}^{-1}$  for the individual exclusive analyses as well as for the combined study.



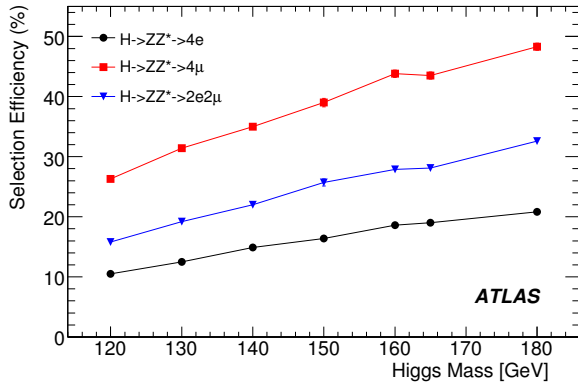
(a)



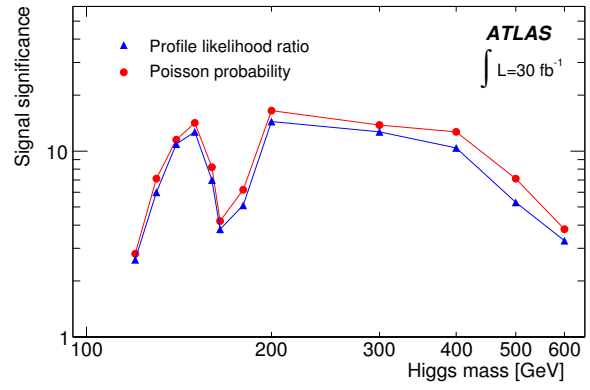
(b)

Figure 9: Expected invariant mass distribution for signal and backgrounds in the  $H \rightarrow 4\ell$  channel based on  $30\text{fb}^{-1}$  for two different Higgs mass values: (a)  $m_H = 130\text{ GeV}$  (b)  $m_H = 180\text{ GeV}$



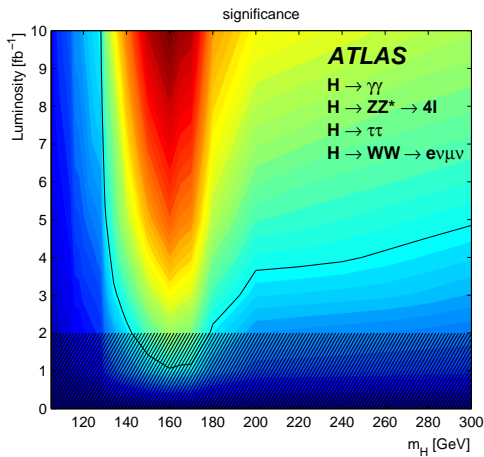


(a)

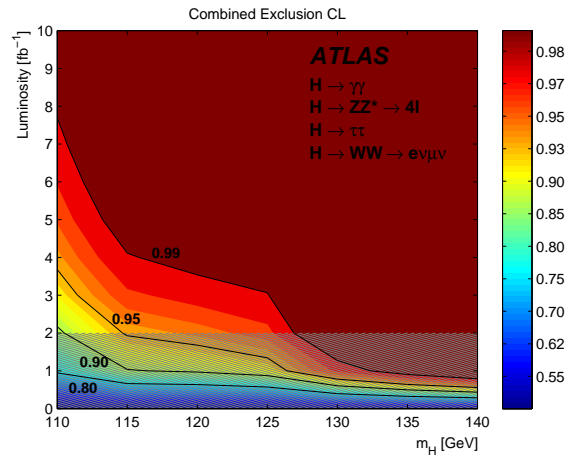


(b)

Figure 10: (a) Expected selection efficiency for  $H \rightarrow 4\ell$  events as a function of the Higgs mass for three different decay sub-channels. (b) Comparison of two different methods to retrieve the signal significance for the  $H \rightarrow 4\ell$  channel as a function of the Higgs mass based on  $30\text{fb}^{-1}$



(a)



(b)

Figure 11: (a) Significance contours for different Standard Model Higgs masses and integrated luminosities. The thick curve represents the  $5\sigma$  discovery contour. The median significance is shown with a colour according to the legend. The hatched area below  $2\text{fb}^{-1}$  indicates the region where the approximations used in the combination are not accurate, although they are expected to be conservative. (b) The expected luminosity required to exclude a Higgs boson with a mass  $m_H$  at a confidence level given by the corresponding colour. The hatched area below  $2\text{fb}^{-1}$  indicates the region where the approximations used in the combination are not accurate, although they are expected to be conservative.